Nevison Cynthia (Orcid ID: 0000-0002-7157-092X)

Journal: Ecological Applications

Manuscript type: Article

Nitrification, denitrification, and competition for soil N: Evaluation of two earth system models against observations

Cynthia Nevison[1,5], Peter Hess[2], Christine Goodale[3], Qing Zhu[4] and Julius Vira[2,6]

[1] University of Colorado, Boulder, Institute for Arctic and Alpine Research, Boulder, Colorado, 80305 USA

[2] Department of Biological and Environmental Engineering, Cornell University, Ithaca, New York, 14583, USA.

[3] Department of Ecology and Evolutionary Biology, Cornell University, Ithaca, New York, 14583, USA.

[4] Lawrence Livermore National Laboratory, Berkeley, California, USA

[5] Corresponding author. E-mail: Cynthia.Nevison@colorado.edu

[6] Present address: Finnish Meteorological Institute, Helsinki, Finland.

Manuscript received 28 October 2020; revised 5 March 2021; accepted 21 April 2021.

Handling Editor: David S. Schimel

Open Research: ELM global output data (Zhu 2021) are available in Zenodo: **https://doi.org/10.5281/zenodo.5590308**. CLM global output data (Danabasoglu 2019) are available from the Earth System Grid Federation at: http://doi.org/10.22033/ESGF/CMIP6.7646.

Abstract

Earth System Models (ESMs) have implemented nitrogen (N) cycles to account for N limitation on terrestrial carbon uptake. However, representing inputs, losses and recycling of N in ESMs is challenging. Here, we use global rates and ratios of key soil N fluxes, including nitrification, denitrification, mineralization, leaching, immobilization and plant uptake (both NH_4^+ and NO_3^-), from the literature to evaluate the N cycles in the land model components of two ESMs. The two land models evaluated here, ELMv1-ECA and CLM5.0, originated from a common model but have diverged in their representation of plant/microbe competition for soil N. The models predict similar global rates of gross primary productivity (GPP) but have ~2 to 3-fold differences in their underlying global mineralization, immobilization, plant N uptake, nitrification and denitrification fluxes. Both models dramatically underestimate the immobilization of NO_3^- by soil bacteria compared to literature values and predict dominance of plant uptake by a single form of mineral nitrogen (NO_3^- for ELM, with regional exceptions, and NH_4^+ for CLM5.0). CLM5.0 strongly underestimates the global ratio of gross nitrification:gross mineralization and both models likely substantially underestimate the ratio of nitrification:denitrification. Few experimental data exist to evaluate this last ratio, in part because nitrification and denitrification are quantified with different techniques and because denitrification fluxes are difficult to measure at all. More observational constraints on soil nitrogen fluxes like nitrification and denitrification, as well as greater scrutiny of the functional impact of introducing separate NH_4^+ and NO_3^- pools into ESMs, could help improve confidence in present and future simulations of N limitation on the carbon cycle.

Key Words

Earth System Models, denitrification, nitrification, nitrogen cycle, nitrogen limitation,

Introduction

Coupled carbon-climate models have been faulted for overestimating the capacity of the land biosphere to absorb fossil CO_2 by neglecting nitrogen (N) limitation [e.g., *Hungate et al.*, 2003; *Zaehle et al.* 2014; *Wieder et al.* 2015]. However, model simulations of N limitation are challenged by the complexity of the N cycle and by limited understanding of plant-soil-microbial competition for N [e.g., *Thomas et al.* 2015; *Zhu et al.* 2017; *Sulman et al.* 2019]. The soil dynamics governing N limitation of the terrestrial carbon (C) cycle are intricately related to multiple processes, including soil N mineralization, immobilization, nitrification and denitrification. Accurate representation of these processes is important for credible future projections of the coupled C-N cycle and the ability of terrestrial ecosystems to sequester fossil carbon.

Experimental data are commonly used to parameterize N cycle processes in global land models [*Cleveland et al.*, 1999; *Del Grosso et al.*, 2000; *Parton et al.*, 2001; *Kattge et al.*, 2009]. However, these parameterizations are based on observed relationships, often from laboratory incubations, at a limited number of sites, which are assumed to apply globally without post hoc evaluation of that assumption. Furthermore, while experimental data have been used to evaluate some aspects of modeled C-N cycling, such as NO_3^- leaching or effects on plant growth, they are seldom used to evaluate mineralization,

immobilization and nitrification [*Zaehle et al.*, 2010; *Thomas et al.*, 2013a; *Zhu et al.*, 2017; *Cheng et al.*, 2019; *Wieder et al.,* 2019].

Experimental approaches toward quantifying mineralization, immobilization and nitrification have evolved over time, with an expansion from a focus on net fluxes measured using "buried bag" techniques to also measuring gross fluxes using isotope (^{15}N) pool dilution techniques [*Schimel and Bennett* 2004]. Buried bag techniques assume that plants are poor competitors for available soil N and can only access the N left over after microbial demands are met. These techniques involve incubating soil cores in a polyethylene bag that prevents NO_3^- leaching losses as well as N uptake by tree roots. The measured net changes in NH_4^+ concentration and NO_3^- concentration within the bag over the incubation period compared to the start are assumed to equal net mineralization and net nitrification, respectively [*Nadelhoffer et al.*, 1983; 1984; *Robertson et al.* 1999].

Isotope (^{15}N) pool dilution studies have challenged the assumptions of buried bag techniques by revealing substantial rates of gross mineralization and gross nitrification in systems without obvious or evident net accumulation of mineral N in either oxidized (NO_3^-) or reduced (NH_4^+) form [*Davidson et al.* 1992, *Hart et al.* 1994*b*, *Neill et al.* 1999]. Isotope dilution, which is described in more detail below, involves small additions of ^{15}N to a pair of soil cores, and observation of the change in ^{15}N composition of the inorganic N pool between an initial and incubated core.

Denitrification is an additional land model output that is rarely evaluated against observations. Denitrification is inherently challenging to measure due to its high degree of spatial and temporal heterogeneity. Furthermore, its end product N_2 composes most of the atmosphere, making it impossible to directly detect the resulting small increases in N_2 concentrations [*Groffman et al.*, 2006; *Morse et al.*, 2015a,b]. N_2O, an intermediate gas produced during denitrification, is more easily and commonly measured than N_2. However, N_2O is also produced by nitrification but the mechanism of N_2O production is not discernible by conventional flux chamber methods [e.g., *Groffman et al.*, 2006; *Burgin and Groffman*, 2012; *Wieder et al.*, 2011]. Consequently, N_2O fluxes are not necessarily a reliable metric of the underlying nitrification and denitrification fluxes, especially since uncertain assumptions must be made about the percent N_2O yield of each process [*Del Grosso et al.*, 2000; *Xu-Ri and Prentice*, 2008]. However, new experimental techniques may allow N_2O fluxes due to nitrification and denitrification to be more easily distinguished [*Ibraim et al.*, 2020].

Among all the ESMs participating in the fifth phase of the Coupled Model Intercomparison Project (CMIP5), only two had land model components that attempted to represent nitrogen limitation on terrestrial C–N biogeochemistry: the Community Earth System Model (CESM) [*Thornton et al.,* 2009; *Koven et al.,* 2013] and the Norwegian Earth System Model-ME (NorESM1) [*Tjiputra et al.,* 2013]. Both CESM and NorESM1 used the Community Land Model (CLM) version 4.0 [*Thornton et al.,* 2009] as their terrestrial ecosystem model. Both predicted substantially lower net C uptake and storage compared to the full suite of carbon-only climate models [*Wieder et al.*, 2015, 2019].

CLM4.0 was an early version of CLM that did not distinguish between NH_4^+ and NO_3^- pools or explicitly model nitrification. Model evaluations to date for CLM4.0 and its successors (CLM4.5 and CLM5.0) indicate that this model overestimates losses of N to denitrification while underestimating loss of N to leaching [*Thomas et al.* 2013a; *Houlton et al.* 2015; *Cheng et al.* 2019].

In this paper, we review the scientific literature for ratios between mineralization, immobilization, nitrification, denitrification, leaching and plant uptake, and how these fluxes are partitioned between the two major mineral N species, NO_3^- and NH_4^+. We focus primarily on flux ratios rather than individual fluxes to better examine fundamental relationships among fluxes and because individual flux magnitudes vary widely across different ecosystems and overall global flux totals are not well known. We compare the observed ratios to output from two ESM land model components, ELMv1-ECA and CLM5.0, both of which evolved from CLM4.5. This exercise reveals some major discrepancies between model and observations, particularly with respect to nitrification and microbial NO_3^- assimilation.

Methods

Definition of fluxes and observational data

Our literature search for observed soil N fluxes and flux ratios was focused on mineralization, immobilization, nitrification, denitrification, leaching and plant uptake, and the partitioning of these fluxes between the two major mineral N species, NO_3^- and NH_4^+ (Figure 1). We use the conventional definitions of gross mineralization as the release of NH_4^+ from organic matter during soil decomposition; immobilization (also

called assimilation) as the uptake of NO_3^- or NH_4^+ by decomposing microbes, generally during the conversion of plant litter into soil organic matter; gross nitrification as the oxidation under aerobic conditions of NH_4^+ to NO_3^-, largely by autotrophic bacteria, who gain their energy from this reaction; and denitrification as the heterotrophic reduction of NO_3^- to N_2, N_2O and other gaseous forms, resulting in loss of fixed N from soil. Denitrification is carried out under low-oxygen conditions by bacteria that use organic carbon as their energy source. We also consider gross primary production (GPP), a carbon flux defined as the amount of CO_2 fixed by plants into organic carbon (minus their autotrophic respiration needs), which we use to sort model nitrogen fluxes into higher and lower productivity grids.

Many of our observational N flux ratios were taken from the isotope (^{15}N) pool dilution meta-analysis of *Booth et al.* [2005]. Isotope dilution involves small additions of ^{15}N to a pair of soil cores, and observation of the change in ^{15}N composition of the extractable inorganic N pool between an initial and incubated core, as production of unlabeled (^{14}N) from mineralization or nitrification dilutes the initial ^{15}N label. The method requires assumptions that gross rates remain constant throughout the assay and that no significant recycling of labeled N into the substrate pool occurs. Gross and net mineralization rates of NH_4^+ are computed using the isotope dilution model of *Kirkham and Bartholomew* [1954]. Immobilization of NH_4^+ is calculated as the difference between gross and net mineralization. Similar equations are used to estimate gross and net nitrification and immobilization of NO_3^- [*Davidson et al.*, 1992].

The meta-analysis of *Booth et al.* [2005] assembled data on gross nitrification, mineralization and immobilization from 100 isotope dilution studies conducted in forest, shrubland, grassland, and agricultural land, representing a wide variety of ecosystems. Booth *et al.* made scatterplots of various log-transformed fluxes and used the regression slopes to quantify the relationships (i.e., ratios) between fluxes. In most cases, a single ratio was reported without error bars, although the scatterplots indicated a substantial range of uncertainty in the flux relationships. Booth *et al.* did not attempt to estimate global annual mean mineralization, nitrification or immobilization fluxes, suggesting these global totals are not well known. We assumed that their flux ratios could be fairly compared to the global model results from the ESMs described below, although their dataset may not have represented all ecosystems, e.g., tropical forests, in proportion to their relative global abundance. Another important caveat is that isotope dilution experiments are carried out in soil cores (i.e., with no competition from plant uptake), whereas plants compete with microbes for mineral N in the ESM results.

We also considered the two primary N loss pathways from soil, leaching and denitrification, in our literature search. Common techniques to measure denitrification empirically include (1) acetylene-based methods, (2) ^{15}N tracers, (3) direct N_2 quantification in the lab, (4) N_2:Ar ratio quantification, and (5) mass balance approaches [*Groffman et al.*, 2006]. All of these methods have their own set of strengths and weaknesses. Globally, bottom-up estimates of terrestrial denitrification amount to ~ 100 TgN/yr, although with high uncertainty [*Galloway et al.*, 2004; *Gruber and Galloway*, 2008]. Our literature search yielded only limited information about global flux ratios involving denitrification, due to the inherent difficulties of measuring

denitrification. Concurrently measured nitrification:denitrification ratios were particularly difficult to find. However, the ratio of nitrification:denitrification is easily computed from land model output and is a potentially useful metric of the relative rate of recycling vs. loss of NO_3^- (Figure 1).

Leaching, defined as the loss of soluble NO_3^- from soil to groundwater, streams and rivers, is more readily measured than denitrification, based on regular monitoring of streamflow and dissolved N concentrations in streams and rivers [*Kroeze and Seitzinger*, 1998; *Seitzinger et al.*, 2005; *Yanai et al.*, 2013]. Bottom-up extrapolation of such measurements yields global leaching estimates on the order of 100 Tg N/yr, which, when combined with (highly uncertain) bottom-up estimates of denitrification, gives a global denitrification: NO_3^- leaching ratio in the range of 1:1 [e.g., *Galloway et al.*, 2004]. *Houlton and Bai* [2009] proposed an alternative method based on isotopic data to estimate the global denitrification: leaching ratio, obtaining a value of 0.5. Their ratio suggests that (only) ~1/3 of N lost from the non-agricultural terrestrial biosphere is denitrified, implying that the other ~2/3 is lost through leaching. Note that the *Houlton and Bai* [2009] definition of N leaching also includes organic and particulate N leaching, which may account for more than half of all N leaching [*Seitzinger et al.*, 2005; *Thomas et al.*, 2015]. However, only NO_3^- leaching is represented in the two land models considered here.

Two additional N fluxes considered in our study, plant uptake of NH_4^+ and NO_3^-, are difficult to measure directly. Total plant N uptake is commonly estimated by measuring

components of plant NPP, then multiplying by the N concentration of each tissue [*Whittaker et al.* 1979]. Other techniques, which allow for the distinction between NO_3^- and NH_4^+ uptake, include adding alternatively $^{15}NH_4^+$ or $^{15}NO_3^-$ fertilizer to soil and measuring the accumulation of ^{15}N in plant tissues [*Daryanto et al*., 2018]. These studies have found wide variability in plant preference for NH_4^+ vs. NO_3^-, depending on plant type and other environmental parameters [*Zhang et al.*, 2018]. In principle, plant uptake of NH_4^+ is more energetically efficient than uptake of NO_3^-, since NH_4^+ can be directly incorporated into glutamate, whereas NO_3^- must be reduced before assimilation. Conversely, NO_3^- is generally considered to be more mobile in soil and thus potentially more accessible to plants, although this is not necessarily true in N-limited conditions where NO_3^- levels are low [*Wang and Macko*, 2011].

Model analysis

Historical simulations of the ELMv1-ECA and CLM5.0 land models were run from 1850-2010, using historical N deposition [*Lamarque et al.* 2005], atmospheric CO_2 forcing from Mauna Loa and land use change (without agricultural N inputs) [*Lawrence et al.*, 2019; *Zhu et al.*, 2019]. The mean and standard deviation of the last 11 years (2000-2010) of these historical simulations were used to approximate present-day condition of the modeled N cycle. Meteorological forcing for both ELM and CLM5.0 came from the Global Soil Wetness Project (GSWP3 version 1, http://hydro.iis.u-tokyo.ac.jp/GSWP3/), with forcing data available from 1901-2010 and cycled over 1901-1920 for years prior to 1901. To initialize the historical simulations, each model was spun up to steady state in 1850 using accelerated decomposition techniques and fixed preindustrial CO_2, land use and atmospheric N deposition [*Lawrence et al.*, 2019]. Simulated N fluxes were sampled

including gross mineralization, gross nitrification, denitrification, leaching, immobilization and plant uptake, with the latter two fluxes partitioned into NH_4^+ and NO_3^-. The linearity of relationships among the above fluxes was analyzed based on scatterplots of global annual mean data, one flux plotted against another. Where possible, key global flux ratios, e.g., gross nitrification:gross mineralization, were calculated based on the slope of a Deming regression fit to the scatterplot [*Nagy*, 2020]. The Deming regression is similar to a standard least squares regression but assigns the same uncertainty to the X and Y axis variables, rather than assuming all error is in the Y variable. When the flux relationships were not linear, the ratio of the total global fluxes was calculated as an alternative metric. Finally, the model flux ratios were compared to available measurements from the literature [*Booth et al.*, 2005].

Community Land Model v. 4.5, common ancestor

The Community Land Model (CLM) is the terrestrial component of the Community Earth System Model (CESM). The coupled carbon/nitrogen cycle was introduced into CLM by *Thornton et al.*, [2002], with various updates over the years [*Thornton and Rosenbloom*, 2005; *Thornton et al.*, 2009]. The updates include a major revision by *Koven et al.* [2013] to create CLM-BGC (biogeochemistry) v4.5, which resolves soil biogeochemistry vertically and separates soil mineral nitrogen into explicit NH_4^+ and NO_3^- pools. CLM-BGC v4.5 is the common ancestor of both models used in the current study, CLM v5.0 and ELMv1-ECA.

ELMv1-ECA

ELMv1-ECA is the terrestrial land model component of the E3SM earth system model [*Golaz et al.*, 2019; *Zhu et al.*, 2019]. ELMv1-ECA has departed from its parent model CLM-BGC 4.5 in various ways, but particularly with respect to the treatment of soil C-N biogeochemistry. ELMv1-ECA represents below-ground nutrient competition between plants, soil microbes and mineral surfaces using the Equilibrium Chemistry Approximation (ECA), a functional coupling strategy to represent the multiple-consumer, multiple-substrate competition network composed of plant roots, soil microbes, and abiotic protection mechanisms [*Tang and Riley*, 2013; *Zhu et al.*, 2017; *Medvigy et al.*, 2019]. The ECA scheme explicitly represents root traits that control nutrient acquisition, including root nutrient carrier enzyme kinetics; activation and deactivation of nutrient carrier enzymes controlled by plant nutritional level; direct plant competition with other soil microbes; and nutrient carrier enzyme-mediated resource uptake preference for NH_4^+ and NO_3^-. ELM includes nutrient limitation as part of a generic dynamic allocation scheme based on water, light, N and phosphorus (P) availability. The model uses flexible plant C:N:P nutrient stoichiometry, including dynamic leaf C:N stoichiometry, with regulation of root nutrient uptake that maintains plant tissue nutritional levels within the range of observed natural variability [*Zhu et al., 2020*]. Since the variables pertaining to plant uptake and microbial immobilization of NH_4^+ and NO_3^- were vertically resolved in ELM output, we integrated these over the soil column for our analysis.

CLM v5.0

In contrast to ELMv1-ECA, soil decomposition processes and plant/microbe competition are relatively unchanged in CLM5.0 with respect to CLM4.5. Both versions of CLM use an equal competition scheme in which potential rates of nitrification, plant uptake and microbial immobilization of NH_4^+ at each soil depth are computed and then reduced proportionally to match available mineral NH_4^+ [*Zhu et al.*, 2017]. Next, potential rates of denitrification, plant uptake and microbial immobilization of NO_3^- are computed and reduced proportionally to match available NO_3^-. Finally, any remaining residual NO_3^- becomes available for leaching, in an algorithm dependent on soil dissolved NO_3^- concentration, surface runoff and subsurface drainage.

However, CLM5.0 also differs from CLM4.5 in multiple ways, including with respect to its representation of soil and plant hydrology, agriculture, and plant N uptake [*Badger and Dirmeyer*, 2015; *Levis et al.*, 2016; *Ghimire et al.*, 2016; *Lawrence et al.*, 2019]. Of particular interest for our study, the treatment of biological nitrogen fixation has been overhauled to incorporate the Fixation and Update of Nitrogen (FUN) model [*Fisher et al.*, 2010; *Shi et al.*, 2016]. FUN is predicated on the concept that N uptake requires the expenditure of energy in the form of carbon, and that plants will select among various potential sources of N for those that are most energetically efficient. FUN calculates the rate of symbiotic N_2 fixation and delivers this N directly to the plant, bypassing the mineral N pool. It also calculates a separate free living N_2 fixation flux based on ecosystem evapotranspiration that is delivered to the soil NH_4^+ pool, following the old CLM4.5

scheme. Plant uptake of NH_4^+ and NO_3^- in FUN is quantified with a new set of variables that distinguish active uptake via symbiotic N_2 fixation versus non-mycorrhizal uptake.

Results

ELMv1-ECA (hereafter referred to as ELM) and CLM5.0 (hereafter referred to as CLM) have very similar global rates of GPP, N_2 fixation and N deposition (Table 1). In contrast they have substantial (~ 2-fold) differences in their rates of gross mineralization (1322 and 2317 Tg N/yr), immobilization (874 and 1550 Tg N/yr) and total plant N uptake (375 and 887 Tg N/yr) (Table 1). Immobilization occurs almost entirely via NH_4^+ in both models. Plant N uptake is also highly polarized toward a single form of inorganic N in the two models, but to opposite forms (Tables 1). The large majority of plant uptake in CLM occurs via NH_4^+, whereas NO_3^- dominates plant uptake in ELM in most ecosystems, with a notable exception in the tropics, where NH_4^+ dominates (Figure 2a,b). In comparison, the available experimental data are variable and suggest that plants can prefer either mineral N species, depending on plant type and environmental conditions [*Daryanto et al.*, 2018; *Zhang et al.*, 2018]. Zhang *et al.* noted that plants originating from strongly acidic soils, such as in the humid subtropics, tend to prefer NH_4^+, but that plants originating from alkaline soils, such as in arid and semi-arid regions, tend to prefer NO_3^-.

The models differ in their absolute gross nitrification rates, with ELM exceeding CLM by a factor of 3 (Table 1). They also differ in the fraction of NH_4^+ produced by gross mineralization that is subsequently nitrified (Figures 2c,d). ELM predicts that 37% of gross mineralization is nitrified (Table 2, Figure 1), with a positive, mainly linear

relationship between gross nitrification and gross mineralization in grids with lower GPP, but a nonlinear relationship at higher GPP. This nonlinearity is largely due to productive tropical regions where less than 10% of gross mineralization is nitrified (Figure 2c; 3a). CLM predicts that only 7% of gross mineralization is nitrified on global average, with little distinction between the tropics and the rest of the world (Table 2, Figure 1). In contrast, the isotope dilution meta-analysis of *Booth et al.* [2005] found that gross nitrification was a non-linear function of gross mineralization ranging from 63% at low gross mineralization rates to 19% at high gross mineralization rates.

Both ELM and CLM predict a strong linear relationship between NH_4^+ immobilization and gross mineralization (Figure 3a,b). In both models, NH_4^+ immobilization accounts for 67% of gross NH_4^+ mineralization (Figure 1, Table 2). In comparison, the observed NH_4^+ gross immobilization:gross mineralization relationship is also strong and linear, with a somewhat larger slope of 84% [*Booth et al.*, 2005]. However, these observations are from isotope dilution studies that exclude competition from plant NH_4^+ uptake.

Plants are not insignificant competitors for NH_4^+ compared to microbes in the models, especially CLM. Table 2 shows that nitrification, immobilization and plant uptake account for 37%, 67% and 9% (ELM) and 7%, 67% and 35% (CLM), respectively, of NH_4^+ produced by gross mineralization. (These totals add up to 113% and 109% for ELM and CLM, respectively, because plants and soil bacteria draw from additional sources of NH_4^+, e.g., existing soil reserves, such that NH_4^+ production and consumption are not in exact equilibrium.)

A particularly interesting result in both ELM and CLM is that NO_3^- immobilization is small to negligible (Tables 1) and accounts for < 1% and < 4% of NO_3^- produced by nitrification, respectively (Table 2). In contrast, the *Booth et al.* [2005] meta-analysis found that microbial NO_3^- immobilization accounted for about 59% of gross nitrification and that the two fluxes were positively and linearly correlated to NO_3^- production.

Loss to denitrification is the single largest fate of NO_3^- in CLM and is also an important fate in ELM, which has an absolute rate of denitrification more than twice as high as CLM (Table 1). In the most productive ecosystems, such as broadleaf forests and tropical rainforests, the nitrification:denitrification ratio in CLM approaches 1:1, implying nearly 100% of nitrification results in denitrification (Figure 2f). Furthermore, nitrification rates tend to be relatively low in grid cells with high GPP, rarely exceeding 4 $gN/m^2/yr$ (Figure 3d; Appendix S1: Figure S1). Similarly, in ELM the nitrification:denitrification ratio is generally lowest in productive ecosystems, although with a notable exception in tropical South America and a small area of tropical Africa, where the ratio exceeds 10:1 (Figure 2e). This seems to be largely a small denominator effect associated with moderate nitrification rates and low denitrification rates in those regions (Appendix S1: Figure S1). Both models predict large nitrification:denitrification ratios of 10:1 in mountain and desert regions, where absolute rates of both fluxes are low and soils are too dry or depleted in carbon for denitrification to occur (Figure 2e,f; Appendix S1: Figure S1). ELM and CLM nitrification:denitrification ratios are 2.04 and 1.88, respectively, when computed as a scatterplot slope, which de-emphasizes points that cluster near the origin, e.g., mountain and desert regions (Figure 3c,d). When

computed from the simple ratio of global totals, these regions bring up the nitrification:denitrification ratio to 2.7 in ELM and 2.1 in CLM (Table 2), meaning that globally 37% and 47% of nitrification results in denitrification in ELM and CLM, respectively.

Plant uptake accounts for most of the remaining half of NO_3^- produced by nitrification in in both models (Table 2). However, due to the low absolute nitrification flux in CLM, NO_3^- accounts for only a small fraction (~8%) of total plant uptake. In ELM, where the absolute nitrification flux is much larger, plant NO_3^- uptake accounts for about 68% of total plant N uptake (Tables 1 and 2).

Leaching is a relatively minor fate of NO_3^- in both models, accounting for about 10% of nitrification. Again, due to the much higher rates of nitrification in ELM, this translates to absolute fluxes of 50 Tg N/yr and 14 Tg N/yr in ELM and CLM, respectively. Both models predict that denitrification dominates leaching as the major loss mechanism for NO_3^-, by a 3.5:1 and 5:1 ratio in ELM and CLM, respectively (Tables 1 and 2).

Discussion

In principle, the introduction of separate NH_4^+ and NO_3^- pools, linked by nitrification, into land models has led to a more realistic simulation of the nitrogen cycle and its regulation of the carbon cycle. In practice, the ELM and CLM models evaluated in this study predict some surprising results, most notably widely different nitrification:gross

mineralization ratios, neither of which agree well with available observations, near negligible NO_3^- immobilization rates and, lastly, low nitrification:denitrification ratios of close to 2:1. The latter seem at odds with the conceptual understanding of nitrification as mechanism for recycling fixed N through plants and soil vs. denitrification as an external or permanent loss of fixed N from soil.

As noted above, nitrification and denitrification traditionally are measured with very different experimental approaches and denitrification is difficult to measure at all. Consequently, these two fluxes are rarely reported concurrently in the literature, making it difficult to critically evaluate the ELM and CLM results. However, our companion paper [*Nevison et al.*, 2022] based on observations at the Hubbard Brook LTER in New Hampshire, suggests a nitrification:denitrification of 14:1 [*Morse et al*., 2015b; *Durán et al.*, 2016; *Darby et al*., 2020]. Although this value involves a wide range of uncertainty, it supports the conceptual understanding that a recycling flux should be substantially larger than a loss flux. The global denitrification flux predicted by CLM is 74 TgN/y (Table 1), in the same ballpark as previous estimates [*Galloway et al.*, 2004], suggesting the primary reason for the low CLM nitrification:denitrification ratio may be inadequate nitrification (although the true global nitrification rate is not well known). In contrast, the low nitrification:denitrification ratio in ELM may result from some combination of low nitrification and a relatively large (179 TgN/yr) denitrification flux.

The lack of substantial NO_3^- immobilization in both CLM5 and ELM is intriguing, given the two models' very different approaches to plant/microbe competition for inorganic N. Empirical studies have shown that NO_3^- immobilization can be an important pathway for

NO_3^- retention in some ecosystems, such as mature forests [*Davidson et al.*, 1992]. Thus, the surprisingly low microbial NO_3^- immobilization flux in both ELM and CLM may result in excessive loss of NO_3^- through the pathways of leaching and denitrification. The small-to-negligible NO_3^- immobilization fluxes, together with the low nitrification:denitrification ratios in both models, raise questions about whether the introduction of separate NH_4^+ and NO_3^- pools into land models has truly led to a more realistic coupled C-N cycle.

The global ratio of denitrification: NO_3^- leaching also appears at odds with observations in both models, although again observational constraints are scarce. It should be noted that the mechanism of NO_3^- loss (i.e., denitrification vs. leaching) in principle is a separate issue from unrealistic plant and/or immobilizer NO_3^- uptake. Imbalances between denitrification and leaching per se do not necessarily affect the functional influence of inorganic nitrogen on the model carbon cycle. Indeed, *Gerber et al.* [2010] argue that it is not necessary to distinguish leaching and denitrification of NO_3^- to accurately model C-N interactions. However, such imbalances render the two primary inorganic N loss terms difficult to evaluate against observations. Furthermore, the two loss mechanisms are not on equal footing in CLM, since denitrifiers compete directly with plants and immobilizing bacteria for NO_3^- while leaching occurs only when excess NO_3^- remains in soil.

The observational constraints on the denitrification:leaching ratio, while quite uncertain themselves, fall in the range of 0.5 to 1.0 (Table 2). Thus they appear incompatible with the ELM denitrification:leaching ratio of 3.5 and the CLM ratio of 5:1. Previous

evaluations of CLM output have come to a similar conclusion, i.e., that the model overestimates the fraction of fixed N lost from terrestrial ecosystems due to denitrification at the expense of leaching [*Thomas et al.*, 2013a; *Houlton et al.*, 2015].

Our findings provide insight into model/observed discrepancies with respect to retention of N added in fertilization experiments, using various versions of CLM and comparing model results to observed ^{15}N tracer addition studies at northern temperate and boreal forest sites. These studies generally have found that CLM overestimates the fraction of added N recovered in vegetation while underestimating the fraction recovered in soil [*Thornton et al.*, 2009; *Thomas et al.*, 2013a,b; *Cheng et al.,* 2019]. *Thomas et al.,* [2013b] used an earlier model version, CLM4.0, which lacked vertically-resolved soil biogeochemistry and did not explicitly model NO_3^- and NH_4^+ as separate pools, and consequently prescribed denitrification in an ad hoc manner as a fraction of excess soil inorganic N. That study found that CLM4.0 overestimated the responsiveness of aboveground NPP to N additions but ultimately underestimated total ecosystem N retention, particularly in soils, likely because it overestimated the loss of soil N to denitrification.

A more recent study with CLM5.0, which uses an empirically-based parameterization for denitrification of NO_3^- [*Del Grosso et al.*, 2000], found a similar tendency of the model to overestimate the amount of N recovered in plants, by a factor of 2 above observed plant recovery in ^{15}N tracer addition experiments, and correspondingly to underestimate recovery of N in soil [*Cheng et al.*, 2019]. Furthermore, soil N recovery in the model was not due to direct immobilization of added N but rather proceeded indirectly via the

cycling of N through plants, in contrast to the results of tracer studies. Both the *Thomas et al.* [2013b] and *Cheng et al.* [2019] results are consistent with some of the CLM5.0 behaviors described in our study, including excessive denitrification and very low NO_3^- immobilization rates.

It is unclear how strongly the N cycle disparities identified in our study influence the carbon cycle in the two models examined here. ELM and CLM have quite similar global GPP rates (109 and 117 PgC/yr, respectively), despite global rates of nitrification that differ by a factor of 3 and global rates of plant N uptake, immobilization, mineralization and denitrification that differ by about a factor of 2. These differences speak to the fact that the global rates of these N fluxes are not well known. Overall, the ELM vs. CLM comparison suggest that models with different underlying N cycles can yield relatively similar carbon cycle results.

Conclusion

Comparison of soil N flux ratios in two ESM land models against observations reveals some interesting model deficiencies, particularly for processes involving soil NO_3^-. While the two models employ very different strategies for modeling plant/microbe soil N competition, both models dramatically underestimate NO_3^- assimilation by immobilizing bacteria. This may lead to exaggerated alternative fates, particularly denitrification, for NO_3^-. Both models simulate nitrification:denitrification ratios of ~ 2:1, which are likely unrealistically low. In addition, CLM predicts that only 7% of gross mineralization results in nitrification, well below observed values (19-63%), and consequently that NH_4^+

accounts for > 90% of plant uptake. In contrast, ELM predicts that nitrification accounts for 37% of gross mineralization, with the main effect of shifting plant uptake toward dominance by NO_3^- (except in the tropics). These disparate soil N dynamics underlie models that otherwise predict similar rates of GPP.

Our study highlights the need for more observational estimates of soil nitrogen fluxes and flux ratios for evaluating ESMs and improving confidence in their simulation of N limitation on the carbon cycle. We note that certain key fluxes like denitrification are inherently uncertain and difficult to measure directly, while others such as NO_3^- leaching losses to streams and N_2O production are more routinely measured. Model-data comparison of soil N fluxes could prove especially useful for guiding models with respect to the introduction of more sophisticated N cycle dynamics involving separate NH_4^+ and NO_3^- pools. In principle, these new dynamics should improve the simulation of the coupled nitrogen-carbon cycle, but our results suggest that more attention is needed to the actual impact of separate NH_4^+ and NO_3^- pools on ESM results.

Acknowledgment: CDN, PH and JV thank U.S. Department of Energy Award # DE-SC0016606. CDN and CG were supported by the NSF Division of Environmental Biology award 1655784. QZ was supported by the Reducing Uncertainties in Biogeochemical Interactions through Synthesis and Computation (RUBISCO) Scientific Focus Area and Energy Exascale Earth System Modeling (E3SM) Project, which are sponsored by the Earth and Environmental Systems Modeling (EESM) Program under the Office of Biological and Environmental Research of the US Department of Energy

Office of Science. We are grateful to Will Wieder for help with CLM5.0. CLM5.0 is part of the CESM project, which is supported primarily by the National Science Foundation. Computing and data storage resources for this project, including the Cheyenne supercomputer (doi.10.5065/D6RX99HX), were provided by the Computational and Information Systems Laboratory (CIS) at NCAR. NCAR is sponsored by the National Science Foundation.

References

Badger, A.M., and P.A. Dirmeyer. 2015. Climate response to Amazon forest replacement by heterogeneous crop cover. *Hydrol. Earth. Syst. Sci.* **19**:4547- 4557.

Booth, M.S., J.M Stark, and E. Rastetter. 2005. Controls on nitrogen cycling in terrestrial ecosystems: a synthetic analysis of literature data. *Ecological Monographs* **75**: 139-157.

Burgin, A. J. and P. M. Groffman. 2012. Soil O_2 controls denitrification rates and N_2O yield in a riparian wetland. *Journal of Geophysical Research Biogeosciences* **117**:G01010.

Cheng, S. J., P. G. Hess, W.R. Wieder, R.Q. Thomas, K.J. Nadelhoffer, J., Vira, D.L. Lombardozzi, P. Gundersen, I.J. Fernandez, P. Schleppi, M.-C. Gruselle, F. Moldan, and C.L. Goodale. 2019. Decadal fates and impacts of nitrogen additions on temperate forest carbon storage: a data–model comparison. *Biogeosciences* **16**: 2771–2793. https://doi.org/10.5194/bg-16-2771-2019.

Cleveland, C. C., et al. 1999. Global patterns of terrestrial biological nitrogen (N_2) fixation in natural ecosystems. *Global Biogeochem. Cycles* **13**:623–645. doi:10.1029/1999GB900014.

Danabasoglu, Gokhan (2019). NCAR CESM2 model output prepared for CMIP6 LUMIP land-crop-noFert. Earth System Grid Federation. https://doi.org/10.22033/ESGF/CMIP6.7646

Darby, B.A., C.L. Goodale, N.A. Chin, C.B. Fuss, A.K. Lang, S.V. Ollinger, and G.M. Lovett. 2020. Depth patterns and connections between gross nitrogen cycling and soil exoenzyme activity in three northern hardwood forests. *Soil Biology and Biochemistry* **147**:107836.

Daryanto, S., L. Wang, W. Gilhooly III, and P-A Jacinthe. 2018. Nitrogen preference across generations under changing ammonium nitrate ratios. *J. of Plant Ecology* 1-10. doi:10.1093/jpe/rty014.

Del Grosso, S.J., W.J. Parton, A.R. Mosier, D.S. Ojima, A.E. Kulmala, and S. Phongpan. 2000. General model for N_2O and N_2 gas emissions from soils due to denitrification. *Global Biogeochem. Cycles* **14**:1045-1060.

Durán, J., J. L. Morse, P. M. Groffman, J. L. Campbell, L. M. Christenson, C. T. Driscoll, T. J. Fahey, M. C. Fisk, G. E. Likens, J. M. Melillo, M. J. Mitchell, P. H. Templer, and M. A. Vadeboncoeur. 2016. Climate change decreases nitrogen pools and mineralization rates in northern hardwood forests. *Ecosphere* **7**:e01251. 10.1002/ecs2.1251.

Fisher, J. B., S. Sitch, Y. Malhi, R. A. Fisher, C. Huntingford, and S.-Y. Tan. 2010. Carbon cost of plant nitrogen acquisition: A mechanistic, globally applicable model of plant

nitrogen uptake, retranslocation, and fixation. *Global Biogeochem. Cycles* **24**: GB1014, doi:10.1029/2009GB003621.

Galloway, J.N., F.J. Dentener, D.G. Capone, E.W. Boyer, R.W. Howarth, S.P. Seitzinger, G.P. Asner, C.C. Cleveland, P.A. Green, E.A. Holland, D.M. Karl, A.F. Michaels, J.H. Porter, A.R. Townsend, and C.J. Vorosmarty. 2004. Nitrogen cycles: past, present, and future. *Biogeochemistry* **70**:153-226.

Ghimire, B., W. J. Riley, C. D. Koven, M. Mu, and J. T. Randerson. 2016. Representing leaf and root physiological traits in CLM improves global carbon and nitrogen cycling predictions. *J. Adv. Mod. Earth Sys.* **8**:598-613.

Golaz, J.-C., P. M. Caldwell, L. P. Van Roekel, M.R. Petersen, Q. Tang, Q., J. D. Wolfe, et al. 2019. The DOE E3SM coupled model version 1:Overview and evaluation at standard resolution. *Journal of Advances in Modeling Earth Systems* **11**:2089–2129.

Groffman, P.M., M.A. Altabet, J. K. Böhlke, K. Butterbach-Bahl, M.B. David, Mary K. Firestone, A.E. Giblin, T.M. Kana, L.P. Nielsen, and M. A. Voytek. 2006. Methods for measuring denitrification: Diverse approaches to a difficult problem, *Ecol. Appl.* **16**:2091-2122.

Gruber, N., and J. Galloway. 2008. An Earth-system perspective of the global nitrogen cycle. *Nature* **451**:293-296.

Houlton, B. Z., and E. Bai. 2009. Imprint of denitrifying bacteria on the global biosphere. *Proc. Natl Acad. Sci.* **106**:21713–21716.

Houlton, B. Z., , A. R. Marklein, and E. Bai. 2015. Representation of nitrogen in climate change forecasts, *Nat. Clim. Change* **5**:398. https://doi.org/10.1038/nclimate2538, 2015.

Hungate, B., J.S. Dukes, M.R. Shaw, Y. Luo, and C.B Field. 2003. Nitrogen and climate change. *Science* **302**:1512-1513.

Ibraim, E., T. Denk, B. Wolf, M. Barthel, R. Gasche, W. Wanek et al. 2020. Denitrification is the main nitrous oxide source process in grassland soils according to quasi-continuous isotopocule analys is and biogeochemical modeling. *Global Biogeochemical Cycles* **33**: e2019GB006505. https://doi.org/10.1029/2019GB006505

Kattge, J., W. Knorr, T. Raddatz, and C. Wirth. 2009. Quantifying photo- synthetic capacity and its relationship to leaf nitrogen content for global- scale terrestrial biosphere models. *Global Change Biol.* **15**:976–991. doi:10.1111/j.1365-2486.2008.01744.x.

Kirkham, D., and W. V. Bartholomew. 1954. Equations for following nutrient transformation in soil, utilizing tracer data. Proceedings of the Soil Science Society of America **18**:33–34.

Koven, C. D., Riley, W. J., Subin, Z. M., Tang, J. Y., Torn, M. S., Collins, W. D., Bonan, G. B., Lawrence, D. M., and Swenson, S. C. 2013. The effect of vertically resolved soil biogeochemistry and alternate soil C and N models on C dynamics of CLM4. *Biogeosciences* **10**:7109-7131, doi:10.5194/bg-10-7109-2013.

Kroeze, C., and S. P. Seitzinger. 1998. Nitrogen inputs to rivers, estuaries and continental shelves and related nitrous oxide emissions in 1990 and 2050: A global model, *Nutr. Cycl. Agroecosyst*. **52**:195–212.

Lawrence, D. M., R. M. Fisher, C. D. Koven, K. W. Oleson, and S. C. Swenson. 2019. The Community Land Model Version 5: Description of new features, benchmarking, and impact of forcing uncertainty. *Journal of Advances in Modeling Earth Systems*, **11**:4245–4287. https://doi.org/10.1029/2018MS001583

Levis, S., A. Badger, B. Drewniak, C. Nevison, X. Ren. 2016. CLM crop yields and water requirements: avoided impacts by choosing RCP 4.5 over 8.5. *Climatic Change* DOI:10.1007/s10584-016-1654-9.

Medvigy, D., G. Wang, Q. Zhu, W.J. Riley, A.M. Trierweiler, B.G. Waring, ... and J. S. Powers. 2019. Observed variation in soil properties can drive large variation in modelled forest functioning and composition during tropical forest secondary succession. *New Phytologist* **223**:1820-1833.

Morse, J.L, J. Duran, and P.M Groffman. 2015a. Soil denitrification fluxes in a northern hardwood forest: The importance of snowmelt and implications for ecosystem N budgets, *Ecosystems* **18**:520-532.

Morse J.L., J. Duran, F. Beall, E.M. Enanga, I.F. Creed, I. Fernandez, and P.M Groffman. 2015b. Soil denitrification fluxes from three northeastern North American forests across a range of nitrogen deposition. *Oecologia* **177**:17–27.

Nadelhoffer, K. J., J. D. Aber, and J. Melillo. 1983. Leaf-litter production and soil organic matter dynamics along a nitrogen-availability gradient in Southern Wisconsin (USA). *Canadian Journal of Forest Research* **13**:12–21.

Nadelhoffer, K., J.D. Aber and J.M Melillo, 1984, Seasonal patterns of ammonium and nitrate uptake in nine temperate forest ecosystems, *Plant and Soil* **80**:321-335.

Nagy, P. 2020. Deming regression (https://www.mathworks.com/matlabcentral/fileexchange/55056-deming-regression), MATLAB Central File Exchange. Retrieved December 31, 2020.

Nevison, C.D., C. Goodale, P. Hess, W. Wieder, J. Vira and P. Groffman. 2022. Nitrification and denitrification in the Community Land Model compared to observations at Hubbard Brook Forest. *Ecological Applications* in press.

Parton, W. J., E. A. Holland, S. J. Del Grosso, M. G. Hartman, R. E. Martin, A. R. Mosier, D. A. Ojima, and D. S. Schimel. 2001. Generalized Model for NOx and N_2O emissions from soils. *J. Geophys. Res.***106**:17,403-17,419.

Seitzinger, S. P., J. A. Harrison, E. Dumont, A. H. W. Beusen, and A. F. Bouwman. 2005. Sources and delivery of carbon, nitrogen, and phos- phorus to the coastal zone: An overview of Global Nutrient Export from Watersheds (NEWS) models and their application. *Global Biogeochem. Cycles***19**. GB4S01, doi:10.1029/2005GB002606.

Shi, M., J. B. Fisher, E. R. Brzostek, and R. P. Phillips. 2016: Carbon cost of plant nitrogen acquisition: global carbon cycle impact from an improved plant nitrogen cycle in the Community Land Model. *Glob. Change Biol.* **22**:1299-1314.

Tang, J., and W. Riley. 2013. A total quasi-steady-state formulation of substrate uptake kinetics in complex networks and an example application to microbial litter decomposition. *Biogeosciences* **10**:8329–8351. https://doi.org/10.5194/bg-10-8329-2013.

Thomas, R Q, S. Zaehle, P. H. Templer, and C. L. Goodale. 2013a. Global patterns of nitrogen limitation: confronting two global biogeochemical models with observations. *Global Change Biology* **19**:2986–2998.

Thomas, R.Q., G.B. Bonan, and C.L. Goodale. 2013b. Insights into mechanisms governing forest carbon response to nitrogen deposition: a model-data comparison using observed responses to nitrogen addition. *Biogeosciences* **10**:3869-3887.

Thomas, R.Q., E.N.J. Brookshire, and S. Gerber. 2015. Nitrogen limitation on land: how can it occur in Earth system models? *Global Change Biology* **21**:1777–1793. doi: 10.1111/gcb.12813.

Thornton, P. E., et al. 2002. Modeling and measuring the effects of disturbance history and climate on carbon and water budgets in evergreen needleleaf forests. *Agric. For. Meteorol.* **113**:185–222.

Thornton, P. E., and N. A. Rosenbloom, Ecosystem model spin-up: Estimating steady state conditions in a coupled terrestrial carbon and nitrogen cycle model, *Ecol. Modell., 189*, 25– 48, 2005.

Thornton, P., S.C. Doney, K. Lindsay, J.K. Moore, N. Mahowald, J.T. Randerson, I. Fung, J.-F. Lamarque, J.J. Feddema, and Y.-H. Lee. 2009. Carbon-nitrogen interactions regulate climate-carbon cycle feedbacks: results from an atmosphere-ocean general circulation model. *Biogeosciences* **6**:2099-2120.

Tjiputra, J.F., C. Roelandt, M. Bentsen, D.M. Lawrence, T. Lorentzen, J. Schwinger, Ø. Seland, and C. Heinze. 2013. Evaluation of the carbon cycle components in the Norwegian Earth System Model (NorESM). *Geosci. Model Dev.* **6**:301-325.

Wang, L., and S.A. Macko. 2011. Constrained preferences in nitrogen uptake across plant species and environments. *Plant, Cell & Environment* **34**:525 – 534.

Weitzman, J.N., P.M. Groffman, J.L. Campbell, C.T. Driscoll, R.T. Fahey, T.J. Fahey, P.G. Schaberg, and L.E. Rustad. 2020. Ecosystem nitrogen response to a simulated ice storm in a northern hardwood forest. *Ecosystems* **23**:1186-1205.

Whittaker, R.H, G.E. Likens, F.H. Bormann, J.S. Eaton, and T.G. Siccama. 1979. The Hubbard Brook ecosystem study: Forest nutrient cycling and element behavior. *Ecology* **60**:203-220.

Wieder, W.R., C.C. Cleveland and A. Townsend. 2011. Throughfall exclusion and leaf litter addition drive higher rates of soil nitrous oxide emissions from a lowland wet tropical forest. *Global Change Biology* **17**: 3195–3207.

Wieder, W.R., C.C. Cleveland, W.K. Smith, and K. Todd-Brown. 2015. Future productivity and carbon storage limited by terrestrial nutrient availability. *Nature Geoscience* **8**:441-445.

Wieder, W. R., D. M. Lawrence, R. A. Fisher, G. B. Bonan, S. J. Cheng, C. L. Goodale, et al. 2019. Beyond static benchmarking: Using experimental manipulations to evaluate land model assumptions. *Global Biogeochemical Cycles* **33**. https://doi.org/10.1029/2018GB006141.

Xu-Ri, X. and C. Prentice. 2008. Terrestrial nitrogen cycle simulation with a dynamic global vegetation model. *Global Change Biology* **14**: 1745–1764. doi: 10.1111/j.1365-2486.2008.01625.x, 2008.

Yanai, R.D., M. A. Vadeboncoeur, S.P. Hamburg, M.A. Arthur, C.B. Fuss, P. M. Groffman, T.G. Siccama, and C. T. Driscoll. 2013. From missing source to missing sink: long-term changes in the nitrogen budget of a northern hardwood forest. *Environ. Sci. Technol.* **47**:11440-11448.

Zaehle, S., A.D. Friend, P. Friedlingstein, F. Dentener, P. Peylin, M. Schulz. 2010. Carbon and nitrogen cycle dynamics in the O-CN land surface model: 2. Role of the nitrogen cycle in the historical terrestrial carbon balance. *Global Biogeochemical Cycles* **24**. doi:10.1029/2009GB003522.

Zaehle, S., C.D. Jones, B. Houlton, J.-F. Lamarque, and E. Robertson. 2014. Nitrogen Availability Reduces CMIP5 Projections of Twenty-First-Century Land Carbon Uptake. *J. of Climate* **28**:2494-2511.

Zhang, J., Z. Cai, and C. Müller. 2018. Terrestrial N cycling associated with climate and plant-specific N preferences: a review. *European Journal of Soil Science* **69**:488–501.

Zhu, Qing. 2021. ELM Nitrogen cycle [Data set]. Zenodo. https://doi.org/10.5281/zenodo.5590308

Zhu, Q., W. J. Riley, and J. Tang. 2017. A new theory of plant–microbe nutrient competition resolves inconsistencies between observations and model predictions. *Ecological Applications* **27**:875–886.

Zhu, Q., Riley, W. J., Tang, J., Collier, N., Hoffman, F. M., Yang, X., & Bisht, G. (2019). Representing nitrogen, phosphorus, and carbon interactions in the E3SM land model: Development and global benchmarking. *Journal of Advances in Modeling Earth Systems* **11**:2238-2258.

Zhu, Q., Riley, W. J., Iversen, C. M., & Kattge, J. (2020). Assessing impacts of plant stoichiometric traits on terrestrial ecosystem carbon accumulation using the E3SM land model. *Journal of Advances in Modeling Earth Systems* **12**. e2019MS001841.

Table 1. ELM v. CLM5 global N cycle flux totals, mean and standard deviation for 2000-2011

	(Pg C/yr)		(Tg N/yr)	
	ELMv1-ECA	**CLM5.0**	**ELMv1-ECA**	**CLM5.0**
Global C Flux				
GPP	109 ± 2	117 ± 2		
Global N Flux				
N_2 Fixation			96 ± 4	93 ± 1
N Deposition			63 ± 0.4	63 ± 0.4
Gross Mineralization			1322 ± 24	2317 ± 40
Total Plant Uptake			375 ± 7	887** ± 17
NH_4^+ Plant Uptake			121 ± 4	761 ± 16
NO_3^- Plant Uptake			253 ± 5	70 ± 2
Total Immobilization			874 ± 15	1550 ± 22*
NH_4^+ Immobilization			872 ± 14	1582 ± 36*
NO_3^- Immobilization			2 ± 0.4	5.5± 0.8*
Gross Nitrification			486 ± 11	157 ± 5

Denitrification			179 ± 8	74 ± 3
Leaching			50 ± 3	14 ± 1

* Total immobilization is from an archived historical simulation of CLM5.0 averaged over 2000-2010 [*Lawrence et al.*, 2019]. NH_4^+ and NO_3^- immobilization fluxes were not included in the archived output and thus were obtained as vertically-resolved fluxes from a separate 11-year simulation, initialized in 2000 from the archived simulation. These were integrated over the soil column to compute the NH_4^+ and NO_3^- immobilization fluxes reported in Table 2. Their sum, 1587.5 Tg N/yr, is slightly different from the archived total immobilization flux.

** Includes 55 ± 1 TgN/yr fraction of N_2 fixation flux that goes directly to plants (without passing through soil) under FUN scheme.

Table 2. ELM v. CLM5 global N cycle flux ratios based alternatively on the ratio of global annual totals and the Deming correlation slopes of global annual scatterplots

		ELMv1-ECA			CLM5.0		
			Correlation			Correlation	
Flux Ratio	Observed	Global ratios	Slope	R	Global ratios	Slope	R
Gross Nitrification:Gross Mineralization	[a] 0.19-0.63	**0.37**	0.30	0.60	**0.07**	0.05	0.34
NH_4^+ Immobilization: Gross Mineralization	0.84	0.67	**0.67**	**0.98**	0.67	**0.67**	**0.99**
NH_4^+ plant uptake/ Gross mineralization	N/A	**0.09**	0.14	0.75	0.33	**0.37**	**0.92**
NO_3^- Immobilization: Nitrification	0.59	**<0.01**	<0.01		**.036**	0.0	0.0
Nitrification: Denitrification	N/A	2.7	**2.04**	**0.94**	2.1	**1.88**	**0.85**
NO_3^- plant uptake: Nitrification	N/A	0.55	**0.49**	**0.82**	**0.44**	0.48	0.76
NO_3^- plant uptake: Total plant uptake	[b] 0.48-0.81	**0.68**	0.57	0.67	**0.08**	0.05	0.19
Denitrification: NO_3^- leaching	[c] ~0.5	**3.5**	6.4	0.20	**5**	0.86	0.04

Notes. Observations are mean ratios derived from slopes of Deming regressions from *Booth et al.*, [2005] (gross N cycling from ^{15}N pool dilution) unless otherwise noted. The nitrogen flux ratios reported here are quantified alternatively based on the Deming regression slopes of scatterplots of model annual mean fluxes, plotted one against the other, and alternatively, based on the simple ratio of global annual mean results. In general, we prefer the regression slope results, for consistency with *Booth et al.* [2005]

and report those in bold font, while reporting the global ratios in regular font. The flux ratios are generally consistent across the two approaches, except in cases where the correlation coefficient between the two fluxes is weak ($R < 0.8$) or visibly nonlinear, e.g., gross nitrification:gross mineralization in ELM (Figure 3). In such cases, the regression slope is less meaningful and the font weighting scheme is reversed in Table 2 to emphasize the simple ratio of global flux totals.

[a] *Booth et al.*, 2005 reported gross nitrification:gross mineralization as a range of values due to the nonlinearity of the relationship.

[b] *Nadelhoffer et al.*, 1984; *Zhang et al*., 2018.

[c] *Houlton and Bai*, 2009.

Figure Captions

Figure 1. Schematic of coupled carbon-nitrogen cycle, with labeling of principal nitrogen fluxes considered in this study. The orange box around soil NH_4^+ and soil NO_3^- represents total soil inorganic nitrogen. Global annual fluxes for ELM and CLM are given in green and purple font, respectively, both as absolute annual values and (in parentheses) as a percentage of gross N mineralization. N deposition is treated as an external flux in the models but in principle can derive from recycled NO_x and NH_3 emissions.

Figure 2. Comparison of annual mean plant N uptake, as the ratio of NH_4^+:total N uptake (a,b), the ratio of gross nitrification:gross mineralization (c,d), and the ratio of nitrification:denitrification (e,f) in ELM (left column) and CLM (right column).

Figure 3. Scatterplot of annual mean gross nitrification vs. gross mineralization (a,b) and gross nitrification vs. denitrification (c,d) from all model grid points for ELM (left column) and CLM (right column). Data are color-coded, with cyan circles indicating more productive grid cells where GPP > 1.5 kgC/m^2/yr. Red lines and text show linear regression slopes and correlation coefficients. Black curve in c,d shows the 1:1 line.

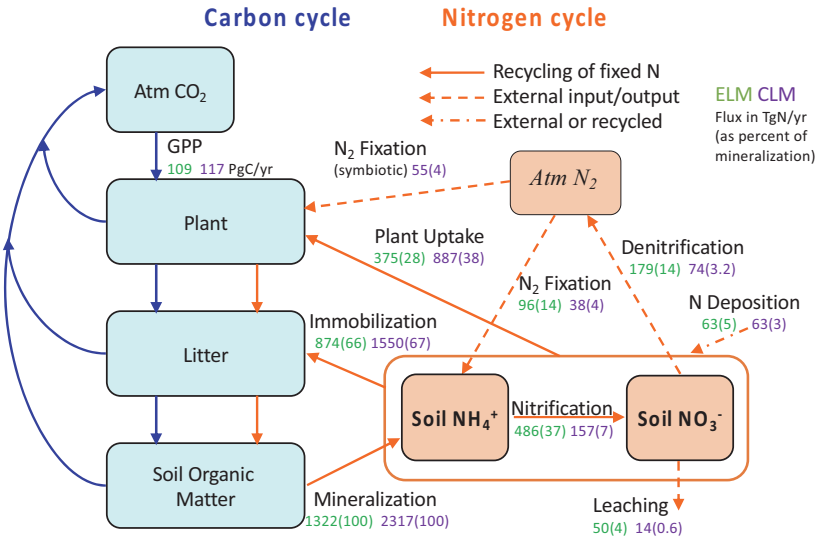

Figure 1.

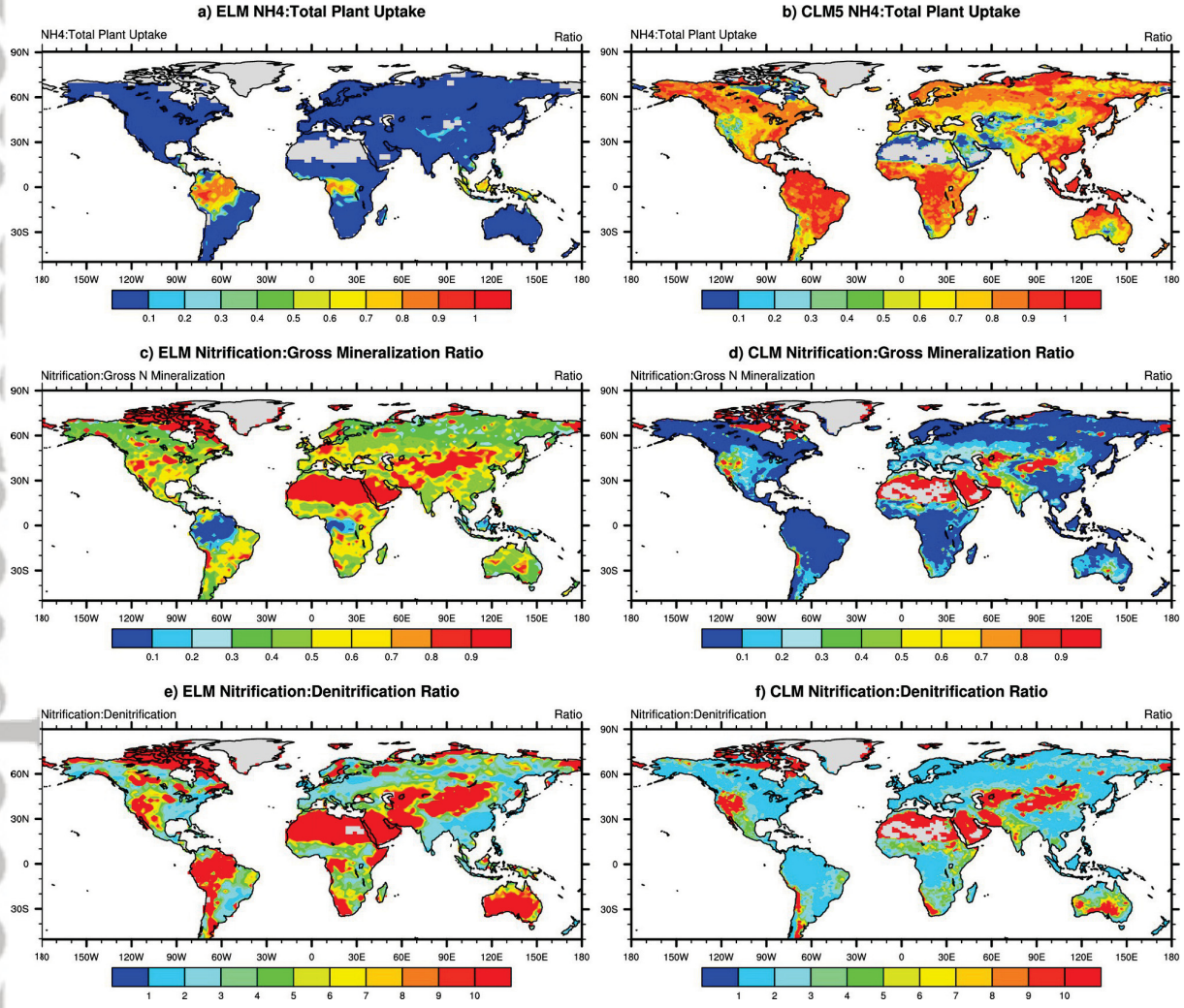

eap_2528_fig2.eps

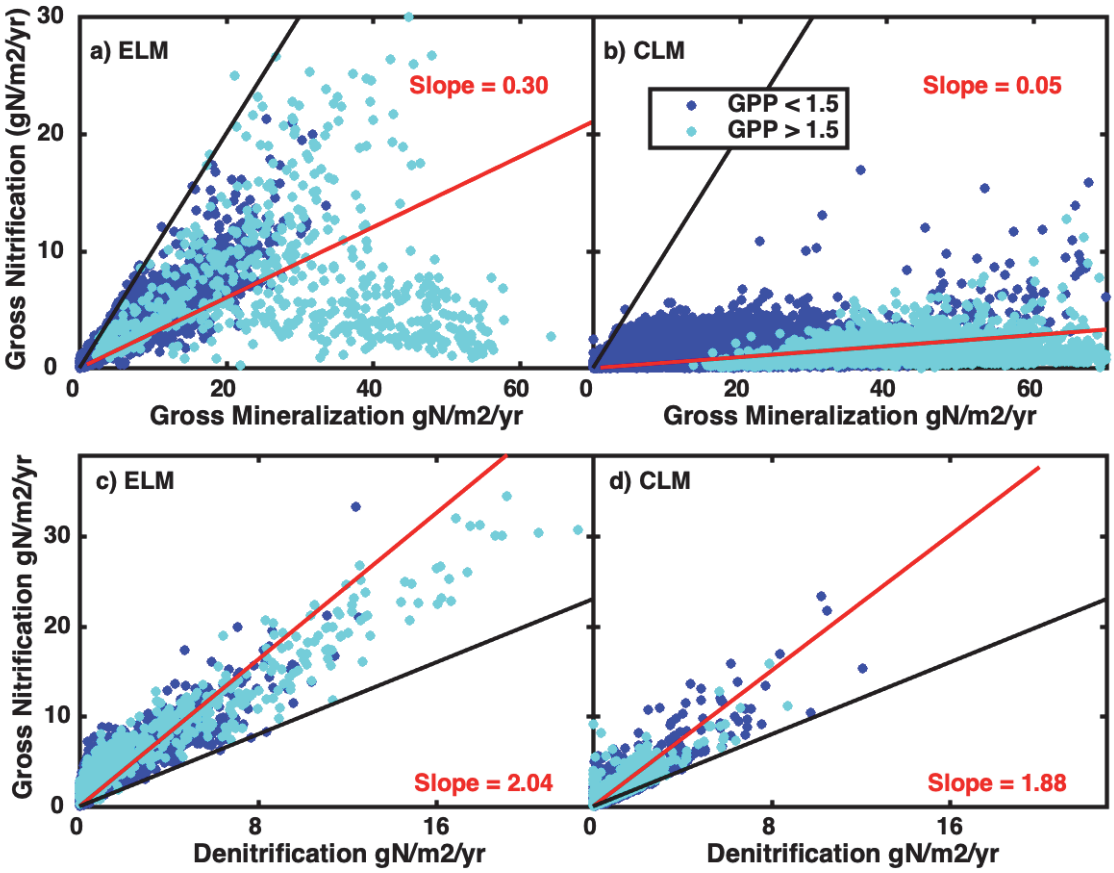

Figure 3.